Search for a Higgs Boson Decaying to Two *W* Bosons at CDF

T. Aaltonen,[24] J. Adelman,[14] T. Akimoto,[56] M. G. Albrow,[18] B. Álvarez González,[12] S. Amerio,[44,y] D. Amidei,[35] A. Anastassov,[39] A. Annovi,[20] J. Antos,[15] G. Apollinari,[18] A. Apresyan,[49] T. Arisawa,[58] A. Artikov,[16] W. Ashmanskas,[18] A. Attal,[4] A. Aurisano,[54] F. Azfar,[43] P. Azzurri,[47,bb] W. Badgett,[18] A. Barbaro-Galtieri,[29] V. E. Barnes,[49] B. A. Barnett,[26] V. Bartsch,[31] G. Bauer,[33] P.-H. Beauchemin,[34] F. Bedeschi,[47] D. Beecher,[31] S. Behari,[26] G. Bellettini,[47,z] J. Bellinger,[60] D. Benjamin,[17] A. Beretvas,[18] J. Beringer,[29] A. Bhatti,[51] M. Binkley,[18] D. Bisello,[44,y] I. Bizjak,[31,ee] R. E. Blair,[2] C. Blocker,[7] B. Blumenfeld,[26] A. Bocci,[17] A. Bodek,[50] V. Boisvert,[50] G. Bolla,[49] D. Bortoletto,[49] J. Boudreau,[48] A. Boveia,[11] B. Brau,[11,b] A. Bridgeman,[25] L. Brigliadori,[59] C. Bromberg,[36] E. Brubaker,[14] J. Budagov,[16] H. S. Budd,[50] S. Budd,[25] S. Burke,[18] K. Burkett,[18] G. Busetto,[44,y] P. Bussey,[22,l] A. Buzatu,[34] K. L. Byrum,[2] S. Cabrera,[17,v] C. Calancha,[32] M. Campanelli,[36] M. Campbell,[35] F. Canelli,[18] A. Canepa,[46] B. Carls,[25] D. Carlsmith,[60] R. Carosi,[47] S. Carrillo,[19,n] S. Carron,[34] B. Casal,[12] M. Casarsa,[18] A. Castro,[6,x] P. Catastini,[47,aa] D. Cauz,[55,dd] V. Cavaliere,[47,aa] M. Cavalli-Sforza,[4] A. Cerri,[29] L. Cerrito,[31,o] S. H. Chang,[28] Y. C. Chen,[1] M. Chertok,[8] G. Chiarelli,[47] G. Chlachidze,[18] F. Chlebana,[18] K. Cho,[28] D. Chokheli,[16] J. P. Chou,[23] G. Choudalakis,[33] S. H. Chuang,[53] K. Chung,[13] W. H. Chung,[60] Y. S. Chung,[50] T. Chwalek,[27] C. I. Ciobanu,[45] M. A. Ciocci,[47,aa] A. Clark,[21] D. Clark,[7] G. Compostella,[59] M. E. Convery,[18] J. Conway,[8] M. Cordelli,[20] G. Cortiana,[44,y] C. A. Cox,[8] D. J. Cox,[8] F. Crescioli,[47,z] C. Cuenca Almenar,[8,v] J. Cuevas,[12,s] R. Culbertson,[18] J. C. Cully,[35] D. Dagenhart,[18] M. Datta,[18] T. Davies,[22] P. de Barbaro,[50] S. De Cecco,[52] A. Deisher,[29] G. De Lorenzo,[4] M. Dell'Orso,[47,z] C. Deluca,[4] L. Demortier,[51] J. Deng,[17] M. Deninno,[6] P. F. Derwent,[18] G. P. di Giovanni,[45] C. Dionisi,[52,cc] B. Di Ruzza,[55,dd] J. R. Dittmann,[5] M. D'Onofrio,[4] S. Donati,[47,z] P. Dong,[9] J. Donini,[59] T. Dorigo,[59] S. Dube,[53] J. Efron,[40] A. Elagin,[54] R. Erbacher,[8] D. Errede,[25] S. Errede,[25] R. Eusebi,[18] H. C. Fang,[29] S. Farrington,[43] W. T. Fedorko,[14] R. G. Feild,[61] M. Feindt,[27] J. P. Fernandez,[32] C. Ferrazza,[47,bb] R. Field,[19] G. Flanagan,[49] R. Forrest,[8] M. J. Frank,[5] M. Franklin,[23] J. C. Freeman,[18] I. Furic,[19] M. Gallinaro,[52] J. Galyardt,[13] F. Garberson,[11] J. E. Garcia,[21] A. F. Garfinkel,[49] K. Genser,[18] H. Gerberich,[25] D. Gerdes,[35] A. Gessler,[27] S. Giagu,[52,cc] V. Giakoumopoulou,[3] P. Giannetti,[47] K. Gibson,[48] J. L. Gimmell,[50] C. M. Ginsburg,[18] N. Giokaris,[3] M. Giordani,[55,dd] P. Giromini,[20] M. Giunta,[47,z] G. Giurgiu,[26] V. Glagolev,[16] D. Glenzinski,[18] M. Gold,[38] N. Goldschmidt,[19] A. Golossanov,[18] G. Gomez,[12] G. Gomez-Ceballos,[33] M. Goncharov,[54] O. González,[32] I. Gorelov,[38] A. T. Goshaw,[17] K. Goulianos,[51] A. Gresele,[44,y] S. Grinstein,[23] C. Grosso-Pilcher,[14] R. C. Group,[18] U. Grundler,[25] J. Guimaraes da Costa,[23] Z. Gunay-Unalan,[36] C. Haber,[29] K. Hahn,[32] S. R. Hahn,[18] E. Halkiadakis,[53] B.-Y. Han,[50] J. Y. Han,[50] F. Happacher,[20] K. Hara,[56] D. Hare,[53] M. Hare,[57] S. Harper,[43] R. F. Harr,[59] R. M. Harris,[18] M. Hartz,[48] K. Hatakeyama,[51] C. Hays,[43] M. Heck,[27] A. Heijboer,[46] J. Heinrich,[46] C. Henderson,[33] M. Herndon,[60] J. Heuser,[27] S. Hewamanage,[5] D. Hidas,[17] C. S. Hill,[11,d] D. Hirschbuehl,[27] A. Hocker,[18] S. Hou,[1] M. Houlden,[30] S.-C. Hsu,[29] B. T. Huffman,[43] R. E. Hughes,[40] U. Husemann,[61] J. Huston,[36] J. Incandela,[11] G. Introzzi,[47] M. Iori,[52,cc] A. Ivanov,[8] E. James,[18] B. Jayatilaka,[17] E. J. Jeon,[28] M. K. Jha,[6] S. Jindariani,[18] W. Johnson,[8] M. Jones,[49] K. K. Joo,[28] S. Y. Jun,[13] J. E. Jung,[28] T. R. Junk,[18] T. Kamon,[54] D. Kar,[19] P. E. Karchin,[59] Y. Kato,[42] R. Kephart,[18] J. Keung,[46] V. Khotilovich,[54] B. Kilminster,[18] D. H. Kim,[28] H. S. Kim,[28] H. W. Kim,[28] J. E. Kim,[28] M. J. Kim,[20] S. B. Kim,[28] S. H. Kim,[56] Y. K. Kim,[14] N. Kimura,[56] L. Kirsch,[7] S. Klimenko,[19] B. Knuteson,[33] B. R. Ko,[17] K. Kondo,[58] D. J. Kong,[28] J. Konigsberg,[19] A. Korytov,[19] A. V. Kotwal,[17] M. Kreps,[27] J. Kroll,[46] D. Krop,[14] N. Krumnack,[5] M. Kruse,[17] V. Krutelyov,[11] T. Kubo,[56] T. Kuhr,[27] N. P. Kulkarni,[59] M. Kurata,[56] Y. Kusakabe,[58] S. Kwang,[14] A. T. Laasanen,[49] S. Lami,[47] S. Lammel,[18] M. Lancaster,[31] R. L. Lander,[8] K. Lannon,[40,r] A. Lath,[53] G. Latino,[47,aa] I. Lazzizzera,[44,y] T. LeCompte,[2] E. Lee,[54] H. S. Lee,[14] S. W. Lee,[54,u] S. Leone,[47] J. D. Lewis,[18] C.-S. Lin,[29] J. Linacre,[43] M. Lindgren,[18] E. Lipeles,[46] A. Lister,[8] D. O. Litvintsev,[18] C. Liu,[48] T. Liu,[18] N. S. Lockyer,[46] A. Loginov,[61] M. Loreti,[44,y] L. Lovas,[15] D. Lucchesi,[44,y] C. Luci,[52,cc] J. Lueck,[27] P. Lujan,[29] P. Lukens,[18] G. Lungu,[51] L. Lyons,[43] J. Lys,[29] R. Lysak,[15] D. MacQueen,[34] R. Madrak,[18] K. Maeshima,[18] K. Makhoul,[33] T. Maki,[24] P. Maksimovic,[26] S. Malde,[43] S. Malik,[31] G. Manca,[30,f] A. Manousakis-Katsikakis,[3] F. Margaroli,[49] C. Marino,[27] C. P. Marino,[25] A. Martin,[61] V. Martin,[22,m] M. Martínez,[4] R. Martínez-Ballarín,[32] T. Maruyama,[56] P. Mastrandrea,[52] T. Masubuchi,[56] M. Mathis,[26] M. E. Mattson,[59] P. Mazzanti,[6] K. S. McFarland,[50] P. McIntyre,[54] R. McNulty,[30,k] A. Mehta,[30] P. Mehtala,[24] A. Menzione,[47] P. Merkel,[49] C. Mesropian,[51] T. Miao,[18] N. Miladinovic,[7] R. Miller,[36] C. Mills,[23] M. Milnik,[27] A. Mitra,[1] G. Mitselmakher,[19] H. Miyake,[56] N. Moggi,[6] C. S. Moon,[28] R. Moore,[18] M. J. Morello,[47,z] J. Morlok,[27] P. Movilla Fernandez,[18] J. Mülmenstädt,[29] A. Mukherjee,[18] Th. Muller,[27] R. Mumford,[26] P. Murat,[18] M. Mussini,[6,x] J. Nachtman,[18] Y. Nagai,[56] A. Nagano,[56] J. Naganoma,[56] K. Nakamura,[56] I. Nakano,[41] A. Napier,[57] V. Necula,[17] J. Nett,[60] C. Neu,[46,w] M. S. Neubauer,[25] S. Neubauer,[27] J. Nielsen,[29,h] L. Nodulman,[2] M. Norman,[10] O. Norniella,[25] E. Nurse,[31]

L. Oakes,[43] S. H. Oh,[17] Y. D. Oh,[28] I. Oksuzian,[19] T. Okusawa,[42] R. Orava,[24] S. Pagan Griso,[44,y] E. Palencia,[18]
V. Papadimitriou,[18] A. Papaikonomou,[27] A. A. Paramonov,[14] B. Parks,[40] S. Pashapour,[34] J. Patrick,[18] G. Pauletta,[55,dd]
M. Paulini,[13] C. Paus,[33] T. Peiffer,[27] D. E. Pellett,[8] A. Penzo,[55] T. J. Phillips,[17] G. Piacentino,[47] E. Pianori,[46] L. Pinera,[19]
K. Pitts,[25] C. Plager,[9] L. Pondrom,[60] O. Poukhov,[16] N. Pounder,[43] F. Prakoshyn,[16] A. Pronko,[18] J. Proudfoot,[2] F. Ptohos,[18,j]
E. Pueschel,[13] G. Punzi,[47,z] J. Pursley,[60] J. Rademacker,[43,d] A. Rahaman,[48] V. Ramakrishnan,[60] N. Ranjan,[49] I. Redondo,[32]
V. Rekovic,[38] P. Renton,[43] M. Renz,[27] M. Rescigno,[52] S. Richter,[27] F. Rimondi,[6,x] L. Ristori,[47] A. Robson,[22] T. Rodrigo,[12]
T. Rodriguez,[46] E. Rogers,[25] S. Rolli,[57] R. Roser,[18] M. Rossi,[55] R. Rossin,[11] P. Roy,[34] A. Ruiz,[12] J. Russ,[13] V. Rusu,[18]
A. Safonov,[54] W. K. Sakumoto,[50] O. Saltó,[4] L. Santi,[55,dd] S. Sarkar,[52,cc] L. Sartori,[47] K. Sato,[18] A. Savoy-Navarro,[45]
P. Schlabach,[18] A. Schmidt,[27] E. E. Schmidt,[18] M. A. Schmidt,[14] M. P. Schmidt,[61,a] M. Schmitt,[39] T. Schwarz,[8]
L. Scodellaro,[12] A. Scribano,[47,aa] F. Scuri,[47] A. Sedov,[49] S. Seidel,[38] Y. Seiya,[42] A. Semenov,[16] L. Sexton-Kennedy,[18]
F. Sforza,[47] A. Sfyrla,[25] S. Z. Shalhout,[59] T. Shears,[30] P. F. Shepard,[48] M. Shimojima,[56,q] S. Shiraishi,[14] M. Shochet,[14]
Y. Shon,[60] I. Shreyber,[37] A. Sidoti,[47] P. Sinervo,[34] A. Sisakyan,[16] A. J. Slaughter,[18] J. Slaunwhite,[40] K. Sliwa,[57]
J. R. Smith,[8] F. D. Snider,[18] R. Snihur,[34] A. Soha,[8] S. Somalwar,[53] V. Sorin,[36] J. Spalding,[18] T. Spreitzer,[34]
P. Squillacioti,[47,aa] M. Stanitzki,[61] R. St. Denis,[22] B. Stelzer,[9,t] O. Stelzer-Chilton,[17] D. Stentz,[39] J. Strologas,[38]
G. L. Strycker,[35] D. Stuart,[11] J. S. Suh,[28] A. Sukhanov,[19] I. Suslov,[16] T. Suzuki,[56] T. Taffard,[25,g] R. Takashima,[41]
Y. Takeuchi,[56] R. Tanaka,[41] M. Tecchio,[35] P. K. Teng,[1] K. Terashi,[51] J. Thom,[18,i] A. S. Thompson,[22] G. A. Thompson,[25]
E. Thomson,[46] P. Tipton,[61] P. Ttito-Guzmán,[32] S. Tkaczyk,[18] D. Toback,[54] S. Tokar,[15] K. Tollefson,[36] T. Tomura,[56]
D. Tonelli,[18] S. Torre,[20] D. Torretta,[18] P. Totaro,[55,dd] S. Tourneur,[45] M. Trovato,[47] S.-Y. Tsai,[1] Y. Tu,[46] N. Turini,[47,aa]
F. Ukegawa,[56] S. Vallecorsa,[21] N. van Remortel,[24,c] A. Varganov,[35] E. Vataga,[47,bb] F. Vázquez,[19,n] G. Velev,[18] C. Vellidis,[3]
V. Veszpremi,[49] M. Vidal,[32] R. Vidal,[18] I. Vila,[12] R. Vilar,[12] T. Vine,[31] M. Vogel,[38] I. Volobouev,[29,u] G. Volpi,[47,z]
P. Wagner,[46] R. G. Wagner,[2] R. L. Wagner,[18] W. Wagner,[27] J. Wagner-Kuhr,[27] T. Wakisaka,[42] R. Wallny,[9] S. M. Wang,[1]
A. Warburton,[34] D. Waters,[31] M. Weinberger,[54] J. Weinelt,[27] W. C. Wester III,[18] B. Whitehouse,[57] D. Whiteson,[46,g]
A. B. Wicklund,[2] E. Wicklund,[18] S. Wilbur,[14] G. Williams,[34] H. H. Williams,[46] P. Wilson,[18] B. L. Winer,[40] P. Wittich,[18,i]
S. Wolbers,[18] C. Wolfe,[14] T. Wright,[35] X. Wu,[21] F. Würthwein,[10] S. M. Wynne,[30] S. Xie,[33] A. Yagil,[10] K. Yamamoto,[42]
J. Yamaoka,[53] U. K. Yang,[14,p] Y. C. Yang,[28] W. M. Yao,[29] G. P. Yeh,[18] J. Yoh,[18] K. Yorita,[14] T. Yoshida,[42] G. B. Yu,[50]
I. Yu,[28] S. S. Yu,[18] J. C. Yun,[18] L. Zanello,[52,cc] A. Zanetti,[55] X. Zhang,[25] Y. Zheng,[9,e] and S. Zucchelli[6,x]

(CDF Collaboration)

[1]*Institute of Physics, Academia Sinica, Taipei, Taiwan 11529, Republic of China*
[2]*Argonne National Laboratory, Argonne, Illinois 60439, USA*
[3]*University of Athens, 157 71 Athens, Greece*
[4]*Institut de Fisica d'Altes Energies, Universitat Autonoma de Barcelona, E-08193, Bellaterra (Barcelona), Spain*
[5]*Baylor University, Waco, Texas 76798, USA*
[6]*Istituto Nazionale di Fisica Nucleare Bologna, University of Bologna, I-40127 Bologna, Italy*
[7]*Brandeis University, Waltham, Massachusetts 02254, USA*
[8]*University of California, Davis, Davis, California 95616, USA*
[9]*University of California, Los Angeles, Los Angeles, California 90024, USA*
[10]*University of California, San Diego, La Jolla, California 92093, USA*
[11]*University of California, Santa Barbara, Santa Barbara, California 93106, USA*
[12]*Instituto de Fisica de Cantabria, CSIC-University of Cantabria, 39005 Santander, Spain*
[13]*Carnegie Mellon University, Pittsburgh, Pennsylvania 15213, USA*
[14]*Enrico Fermi Institute, University of Chicago, Chicago, Illinois 60637, USA*
[15]*Comenius University, 842 48 Bratislava, Slovakia; Institute of Experimental Physics, 040 01 Kosice, Slovakia*
[16]*Joint Institute for Nuclear Research, RU-141980 Dubna, Russia*
[17]*Duke University, Durham, North Carolina 27708, USA*
[18]*Fermi National Accelerator Laboratory, Batavia, Illinois 60510, USA*
[19]*University of Florida, Gainesville, Florida 32611, USA*
[20]*Laboratori Nazionali di Frascati, Istituto Nazionale di Fisica Nucleare, I-00044 Frascati, Italy*
[21]*University of Geneva, CH-1211 Geneva 4, Switzerland*
[22]*Glasgow University, Glasgow G12 8QQ, United Kingdom*
[23]*Harvard University, Cambridge, Massachusetts 02138, USA*
[24]*Division of High Energy Physics, Department of Physics, University of Helsinki and Helsinki Institute of Physics,
FIN-00014, Helsinki, Finland*
[25]*University of Illinois, Urbana, Illinois 61801, USA*

^{26}The Johns Hopkins University, Baltimore, Maryland 21218, USA

^{27}Institut für Experimentelle Kernphysik, Universität Karlsruhe, 76128 Karlsruhe, Germany

^{28}Center for High Energy Physics: Kyungpook National University, Daegu 702-701, Korea;
Seoul National University, Seoul 151-742, Korea;
Sungkyunkwan University, Suwon 440-746, Korea;
Korea Institute of Science and Technology Information, Daejeon, 305-806, Korea;
Chonnam National University, Gwangju, 500-757, Korea

^{29}Ernest Orlando Lawrence Berkeley National Laboratory, Berkeley, California 94720, USA

^{30}University of Liverpool, Liverpool L69 7ZE, United Kingdom

^{31}University College London, London WC1E 6BT, United Kingdom

^{32}Centro de Investigaciones Energeticas Medioambientales y Tecnologicas, E-28040 Madrid, Spain

^{33}Massachusetts Institute of Technology, Cambridge, Massachusetts 02139, USA

^{34}Institute of Particle Physics: McGill University, Montréal, Canada H3A 2T8;
and University of Toronto, Toronto, Canada M5S 1A7

^{35}University of Michigan, Ann Arbor, Michigan 48109, USA

^{36}Michigan State University, East Lansing, Michigan 48824, USA

^{37}Institution for Theoretical and Experimental Physics, ITEP, Moscow 117259, Russia

^{38}University of New Mexico, Albuquerque, New Mexico 87131, USA

^{39}Northwestern University, Evanston, Illinois 60208, USA

^{40}The Ohio State University, Columbus, Ohio 43210, USA

^{41}Okayama University, Okayama 700-8530, Japan

^{42}Osaka City University, Osaka 588, Japan

^{43}University of Oxford, Oxford OX1 3RH, United Kingdom

^{44}Istituto Nazionale di Fisica Nucleare, Sezione di Padova-Trento, University of Padova, I-35131 Padova, Italy

^{45}LPNHE, Universite Pierre et Marie Curie/IN2P3-CNRS, UMR7585, Paris, F-75252 France

^{46}University of Pennsylvania, Philadelphia, Pennsylvania 19104, USA

^{47}Istituto Nazionale di Fisica Nucleare Pisa, University of Pisa, University of Siena and Scuola Normale Superiore, I-56127 Pisa, Italy

^{48}University of Pittsburgh, Pittsburgh, Pennsylvania 15260, USA

^{49}Purdue University, West Lafayette, Indiana 47907, USA

^{50}University of Rochester, Rochester, New York 14627, USA

^{51}The Rockefeller University, New York, New York 10021, USA

^{52}Istituto Nazionale di Fisica Nucleare, Sezione di Roma 1, Sapienza Università di Roma, I-00185 Roma, Italy

^{53}Rutgers University, Piscataway, New Jersey 08855, USA

^{54}Texas A&M University, College Station, Texas 77843, USA

^{55}Istituto Nazionale di Fisica Nucleare Trieste/Udine, University of Trieste/Udine, Italy

^{56}University of Tsukuba, Tsukuba, Ibaraki 305, Japan

^{57}Tufts University, Medford, Massachusetts 02155, USA

^{58}Waseda University, Tokyo 169, Japan

^{59}Wayne State University, Detroit, Michigan 48201, USA

^{60}University of Wisconsin, Madison, Wisconsin 53706, USA

^{61}Yale University, New Haven, Connecticut 06520, USA

We present a search for a Higgs boson decaying to two W bosons in $p\bar{p}$ collisions at $\sqrt{s} = 1.96$ TeV center-of-mass energy. The data sample corresponds to an integrated luminosity of 3.0 fb^{-1} collected with the CDF II detector. We find no evidence for production of a Higgs boson with mass between 110 and 200 GeV/c^2, and determine upper limits on the production cross section. For the mass of 160 GeV/c^2, where the analysis is most sensitive, the observed (expected) limit is 0.7 pb (0.9 pb) at 95% Bayesian credibility level which is 1.7 (2.2) times the standard model cross section.

The Higgs boson in the standard model (SM) breaks the electroweak $SU(2)_L \otimes U(1)_Y$ symmetry. While this symmetry is now well established, the mechanism of the symmetry breaking has not yet been identified. Direct searches at the LEP experiments have set a lower limit on the Higgs boson mass m_H of 114.4 GeV/c^2 at 95% C.L. in the context of the SM [1]. Precision measurements provide the indirect upper limit $m_H < 144$ GeV/c^2 at

95% C.L. through radiative corrections to the SM predictions of the particle masses and couplings [2]. However, these indirect limits assume no significant contributions to the radiative corrections due to as yet unobserved processes.

In this Letter, we report a search for the process $gg \rightarrow H \rightarrow WW^{(*)}$ in a 3.0 fb^{-1} integrated luminosity sample of $p\bar{p}$ collisions at $\sqrt{s} = 1.96$ TeV produced by the Fermilab

Tevatron and collected by the CDF II detector. For a SM Higgs boson with a mass that is not directly excluded by the LEP experiments, the dominant production mechanism at the Tevatron is gluon-gluon fusion which proceeds via a virtual top quark loop [3]. For $m_H > 135$ GeV/c^2, the SM Higgs boson decays primarily to the WW^* [3], where one of the final state W bosons is virtual for m_H below 2 times the W mass.

The events are reconstructed in the $ll\nu\nu$ final state, whose branching fraction is 6.0% of the WW^* decays, where l is either an electron e or a muon μ, including those from τ leptons produced in the W decays. The SM Higgs boson branching fraction to WW^* varies from 7.5% at 115 GeV/c^2 to 73.5% at 200 GeV/c^2 with a maximum of 96.5% at ≈ 170 GeV/c^2 [3]. Previous searches set limits ranging from 10 to 40 times the predicted SM rate, depending on the value of m_H [4].

The CDF II detector is a multipurpose solenoidal spectrometer surrounded by calorimeters and muon detectors [5]. The geometry is described using the azimuthal angle ϕ and the pseudorapidity $\eta \equiv -\ln[\tan(\theta/2)]$, where θ is the polar angle with respect to the proton beam axis (positive z axis). The transverse energy E_T is $E\sin\theta$, where E is the energy associated with a calorimeter element or energy cluster. Similarly, p_T is the track momentum component transverse to the beam line.

The events we consider must pass one of four online selections, triggers, before being recorded. One electron trigger requires an electromagnetic (EM) energy cluster in the central ($|\eta| < 1.1$) calorimeter with $E_T > 18$ GeV matched to a track found in the drift chamber with $p_T > 8$ GeV/c. A second electron trigger requires an EM energy cluster with $E_T > 20$ GeV in the forward ($1.2 < |\eta| < 2.0$) calorimeter and the missing transverse energy $\not{E}_T > 15$ GeV. The variable $\vec{\not{E}}_T$, used to infer the presence of neutrinos, is defined as $\sum_i E_{T,i}\hat{n}_{T,i}$ and $\not{E}_T \equiv |\vec{\not{E}}_T|$, where $\hat{n}_{T,i}$ is the transverse component of the unit vector pointing from the interaction point to calorimeter element i. Muon triggers are based on track segments in the muon chambers matched to a drift-chamber track with $p_T > 18$ GeV/c. Trigger efficiencies are measured using leptonic W and Z data samples [6].

To improve the signal acceptance while maintaining acceptable background rejection for the $W + $ jets and $W\gamma$ processes where a jet or γ is misidentified as a lepton, we use a modified version of the lepton identification strategy developed for the WZ observation analysis [7]. Candidate leptons are separated into six mutually exclusive categories: two for electrons; three for muons; and one for tracks that extrapolate outward to detector regions with insufficient calorimeter coverage for energy measurement. The electron categories are central ($|\eta| < 1.1$) using a drift-chamber-based tracking algorithm and forward ($1.2 < |\eta| < 2.0$) using a silicon-detector-based tracking algorithm. One of the muon categories uses the muon

chambers and the other two use tracks matched with energy deposits consistent with minimum ionization in the central or forward calorimeters.

All lepton candidates are required to be isolated such that the sum of the E_T for the calorimeter elements in a cone of $\Delta R = \sqrt{(\Delta\eta)^2 + (\Delta\phi)^2} < 0.4$ around the lepton is less than 10% of the E_T (for electrons) or p_T (for muons and track lepton candidates). For lepton types in the central region where the track finding efficiency is sufficient, we also apply a track-based isolation criterion which requires there is no more than 10% of the electron E_T or muon p_T in other tracks within a cone of $\Delta R < 0.4$ around the lepton track.

The Higgs boson candidates are selected from events with exactly two lepton candidates. At least one lepton is required to match a trigger lepton candidate and have $E_T > 20$ GeV ($p_T > 20$ GeV/c) for electrons (muons). We loosen this requirement to 10 GeV (GeV/c) for the other lepton to increase the kinematic acceptance, particularly for lower m_H where one W is off shell below the W boson mass and produces a lower p_T lepton. We also require a dilepton invariant mass $m_{\ell\ell} > 16$ GeV/c^2 to suppress misidentified multijet events.

Aside from $H \to WW^{(*)}$ production, other SM processes that can lead to two high-p_T leptons include Drell-Yan (DY), $t\bar{t}$, WW, WZ, and ZZ production, and W production in association with a photon ($W\gamma$) or a jet ($W + $ jets) misidentified as a lepton. The $t\bar{t}$ contribution is suppressed by requiring fewer than two reconstructed jets with $E_T > 15$ GeV and $|\eta| < 2.5$ in the event. The DY background is suppressed by requiring sufficiently large $\not{E}_T$ in the event to remove contributions from mismeasured leptons or jets. This is achieved by requiring $\not{E}_{T,\text{rel}} > 25$ GeV, where $\not{E}_{T,\text{rel}}$ is $\not{E}_T \sin\Delta\phi_{\not{E}_T,(\ell,\text{jet})}$ if $\Delta\phi_{\not{E}_T,(\ell,\text{jet})} < \frac{\pi}{2}$ and $\not{E}_T$ otherwise, and $\Delta\phi_{\not{E}_T,(\ell,\text{jet})}$ is the angle between the $\vec{\not{E}}_T$ direction and the nearest lepton or jet. The observed $\not{E}_T$ is corrected for muons and track-only lepton candidates, because they do not deposit all of their energy in the calorimeter. Except for $W + $ jets, acceptances are determined using data simulated with the MC@NLO program for WW [8], PYTHIA for $H \to WW^{(*)}$, DY, WZ, ZZ, and $t\bar{t}$ [9], and the generator described in Ref. [10] for $W\gamma$.

The response of the CDF II detector is then estimated with a GEANT-4-based simulation [11] to which an efficiency correction of up to 10% per lepton is applied based on measurements of the lepton reconstruction and identification efficiencies using observed $Z \to \ell^+\ell^-$ events. An additional correction is applied to the $W\gamma$ background estimate based on a measurement in data of the photon-conversion veto efficiency. The $W + $ jets contribution is estimated from data by extrapolating from a sample of events that contain an identified lepton and a jet j_l containing a track or EM energy cluster similar to those required in the lepton identification. The contribution of each event to the total yield is scaled by the probability that

the j_l is identified as a lepton. This probability $p(p_T; j_l)$ is determined for each lepton type as a function of the j_l p_T using multijet events collected with jet-based triggers. A correction to $p(p_T; j_l)$ is applied for the small real lepton contribution using Monte Carlo simulation of single W and Z boson production.

Based on the procedure above, we expect 768 ± 91 background events and observe 779 in the selected region. The expected composition of the background is 356 ± 49 WW, 24.9 ± 3.9 WZ, 21.8 ± 3.5 ZZ, 25.5 ± 5.0 $t\bar{t}$, 138 ± 31 DY, 90.5 ± 24.1 $W\gamma$, and 111 ± 27 W + jets, where the indicated uncertainties include the systematic uncertainties described below. As a cross-check of the background model, we measure the fraction of $q\bar{q} \to WW$ events in the sample with a similar method to the signal extraction described below and find it to be consistent with the expectation. Table I shows the dependence of expected yield on m_H. Since the level of non-$WW^{(*)}$ background depends on the lepton identification categories, this information is used to divide the sample into high and low signal-to-background (S/B) classes. The low S/B category largely consists of candidates with a forward lepton.

After selection, the dominant background is the $q\bar{q} \to WW$ process which differs from the signal process only by spin, production mechanism, and resonant structure. Because of the two neutrinos in the final state, a simple mass peak cannot be used to isolate the resonant $gg \to H \to WW^{(*)}$ process from the backgrounds. Instead, we combine two different multivariate techniques to differentiate signal and background. One is a matrix element (ME) technique, which uses an event-by-event calculation of the probability density for each contributing process to produce the observed event. If all details of the collision properties and the detector response are modeled in the ME calculation, this method provides the optimal sensitivity to the signal. However, there are several approximations used in the calculations: theoretical differential cross sections are only implemented to leading order, a simple parameterization of the detector response is used, and for some small (WZ and $t\bar{t}$) or difficult to model (DY) backgrounds, we do not calculate a probability density. In order to improve these approximations, we extend the ME calculation with a neural network (NN) which exploits the more complete model implemented in the simulated data and W + jets model.

The event probability density for the ME method is

$$P(\vec{x}_{\mathrm{obs}}) = \frac{1}{\langle \sigma \rangle} \int \frac{d\sigma_{LO}(\vec{y})}{d\vec{y}} \epsilon(\vec{y}) G(\vec{x}_{\mathrm{obs}}, \vec{y}) d\vec{y},$$

where the elements of $\vec{y}$ ($\vec{x}_{\mathrm{obs}}$) are the true (observed) values of the lepton momenta and $\not{E}_T$, $d\sigma_{LO}/d\vec{y}$ is the parton level differential cross section [12], $\epsilon(\vec{y})$ is a parameterization of detector acceptance and efficiency function, and $G(\vec{x}_{\mathrm{obs}}, \vec{y})$ is the transfer function representing the detector resolution and a PYTHIA-based estimate of transverse momentum of the $\ell\ell\not{E}_T$ system due to the initial state radiation. The constant $\langle \sigma \rangle$ normalizes the total event probability to unity. This calculation integrates the theoretical differential cross section over the missing information due to two unobserved neutrinos in the final state. We form a likelihood ratio discriminant which is the signal probability divided by the sum of signal and background probabilities $LR_{H \to WW^{(*)}}(\vec{x}_{\mathrm{obs}}) \equiv \frac{P_H(\vec{x}_{\mathrm{obs}})}{P_H(\vec{x}_{\mathrm{obs}}) + \sum_i k_i P_i(\vec{x}_{\mathrm{obs}})}$ where k_i are the expected background fractions of WW, ZZ, $W\gamma$, and W + jets. The LR distributions are shown in Fig. 1(a). Additional ME likelihood ratios LR_{WW}, LR_{ZZ}, $LR_{W\gamma}$, and $LR_{W+\mathrm{jets}}$ are defined analogously to $LR_{H \to WW^{(*)}}$.

For the final results, a NN discriminant is used to extend the ME calculation using as input the ME likelihood ratios in addition to various kinematic variables. For each of the Higgs boson masses investigated, a NN is trained on signal events and an appropriately weighted composition of background events. The NN classifies events as signal or background based on the inputs $LR_{H \to WW^{(*)}}$, LR_{WW}, LR_{ZZ}, $LR_{W\gamma}$, $LR_{W+\mathrm{jets}}$, $\Delta\phi_{\ell\ell}$, $\Delta R_{\ell\ell}$, $m_{\ell\ell}$, $\not{E}_T$, $\Delta\phi_{\not{E}_T,(\ell,\mathrm{jet})}$, and $\not{E}_{T,\mathrm{rel}}$, where $\Delta\phi_{\ell\ell}$ and $\Delta R_{\ell\ell}$ are the separation between the two leptons in ϕ and ΔR, respectively. We find that the most discriminating input variables are $LR_{H \to WW^{(*)}}$, $\Delta R_{\ell\ell}$, and $\not{E}_{T,\mathrm{rel}}$. An example of the NN output is shown in Fig. 1(b). The presented results use the NEUROBAYES [13] program. Comparable results are also obtained using the TMVA-MLP [14] program, demonstrating the robustness of the technique.

For the signal and backgrounds modeled by Monte Carlo simulation, the same procedures as Ref. [7] are used to assess the systematic uncertainties on the lepton selection efficiency, trigger efficiency, parton-distribution function, and luminosity to be 1.4% to 2.0%, 2.1% to 7.1%, 1.9%–4.1%, and 6%, respectively, depending on mode. The cross section uncertainties are 10% for WW [12], WZ [12], ZZ [12], and $W\gamma$ [15], and 15% for $t\bar{t}$ [16]. Based on a comparison of simulated WW events generated with MC@NLO and PYTHIA, we assign a systematic uncertainty on the acceptance due to higher order QCD effects of 5.5% for WW events and 10% for the other modes which are only simulated at leading order.

TABLE I. Expected Higgs boson events as a function of m_H.

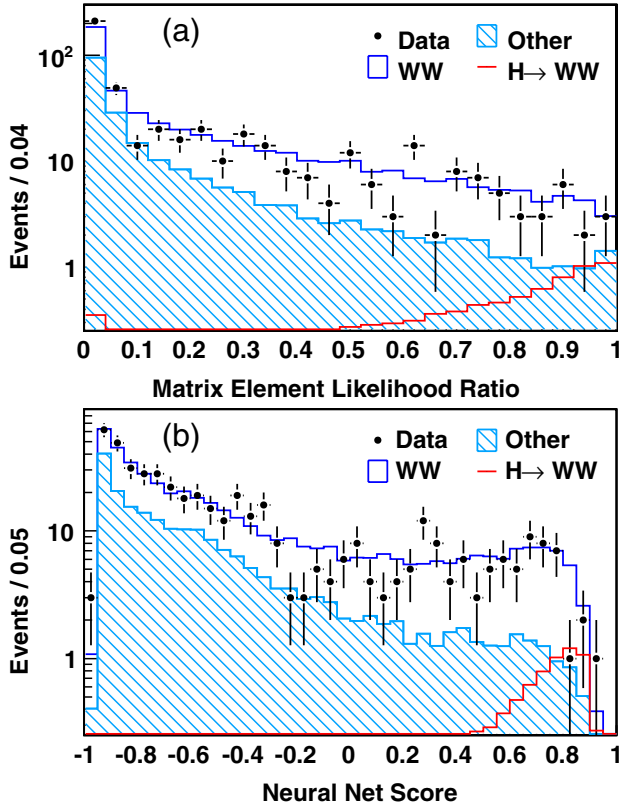| m_H (GeV/c^2)	110	120	130	140	150	160	170	180	190	200
Expected yield	0.5	1.9	4.3	7.0	9.3	11.6	11.0	9.0	6.4	5.1

FIG. 1 (color online). The likelihood ratio distribution from (a) the ME discriminate alone and (b) the full NN score for $m_H = 160$ GeV/c^2. The Higgs boson distribution is normalized to the SM expectation. The distributions are shown only for the high S/B class, which provides the majority of the sensitivity.

The systematic uncertainty on the $W +$ jets background is estimated to be 24% from differences in the observed probability that a jet is identified as a lepton for jets collected using different jet E_T trigger thresholds. These variations correspond to changing the parton composition of the jets and the relative amount of contamination from real leptons. Because only the $\not{E}_{T,\mathrm{rel}}$ requirement suppresses the DY background, there is an uncertainty due to the $\not{E}_T$ resolution modeling, which is estimated to be

20% based on comparisons of the data and Monte Carlo simulation in a sample of dilepton events. For the $W\gamma$ background contribution, there is an additional uncertainty of 20% from the detector material description and photon-conversion veto efficiency.

A Bayesian credibility level (C.L.) is calculated for each m_H hypothesis based on the combined binned likelihood of the discriminant distributions for the high and low S/B samples. A posterior density is obtained by multiplying this likelihood by Gaussian prior densities for the background normalizations and systematic uncertainties leaving $\sigma(gg \to H) \times \mathcal{B}(H \to WW^{(*)})$ with a uniform prior density. A 95% C.L. limit is then determined such that 95% of the posterior density for $\sigma \times \mathcal{B}$ falls below the limit. Limits as a fraction of the SM cross section $\sigma_{\mathrm{SM}}(gg \to H)$ are calculated by including $\sigma_{\mathrm{SM}}(gg \to H)$ as a parameter whose prior density is determined by the 10% theoretical uncertainty of its next-to-next-to-leading-log prediction [17]. The resulting cross section limits for both discriminants are shown in Table II and Fig. 2. Because the NN uses the ME calculation as input, it is the full result; the ME results are given only for comparative purposes.

In conclusion, we have presented limits on the production of a Higgs boson through gluon fusion followed by its decay to a pair of W bosons. A combination of matrix element and neural network techniques is used to discriminate signal from background. Studies using the two techniques independently achieve consistent results with a sensitivity approximately $0.1\sigma_{\mathrm{SM}}$ worse than the combination at $m_H = 160$ GeV/c^2. The consistency of results obtained with different algorithms provides evidence of the robustness of the multivariate techniques. At the most sensitive value of $m_H = 160$ GeV/c^2, the observed limit is 1.7 times the SM prediction where the median expected limit is 2.2, corresponding to a downward fluctuation slightly larger than 1 standard deviation. Compared to an optimized selection and a likelihood based on the $\Delta\phi_{\ell\ell}$ variable, the multivariate discriminators gain a factor of 1.7 to 2.5 in effective integrated luminosity depending on m_H. This measurement also constrains alternative models in which

TABLE II. Expected and observed upper limits on $\sigma(gg \to H) \times \mathcal{B}(H \to WW^{(*)})$ and $(\sigma \times \mathcal{B})/(\sigma \times \mathcal{B})_{\mathrm{SM}}$ for various m_H.

| m_H (GeV/c^2)	110	120	130	140	150	160	170	180	190	200
				Using Matrix Element Only						
Expected (pb)	3.6	2.6	2.2	1.9	1.5	0.9	0.9	1.1	1.2	1.3
Observed (pb)	2.8	1.5	1.1	0.9	0.8	0.7	0.6	0.7	1.0	1.5
Expected/SM	63.7	19.6	9.4	6.0	4.3	2.4	2.6	3.8	6.0	8.2
Observed/SM	50.3	10.9	4.7	3.0	2.3	1.7	1.8	2.6	5.0	10.3
				Using Neural Net Discriminator						
Expected (pb)	3.0	2.3	1.9	1.7	1.4	0.9	0.8	1.0	1.1	1.2
Observed (pb)	2.5	1.7	1.2	1.1	0.9	0.7	0.7	0.7	1.0	1.6
Expected/SM	54.0	17.1	8.4	5.4	3.9	2.2	2.4	3.5	5.6	7.7
Observed/SM	44.6	13.2	5.3	3.5	2.6	1.7	2.2	2.7	5.5	10.6
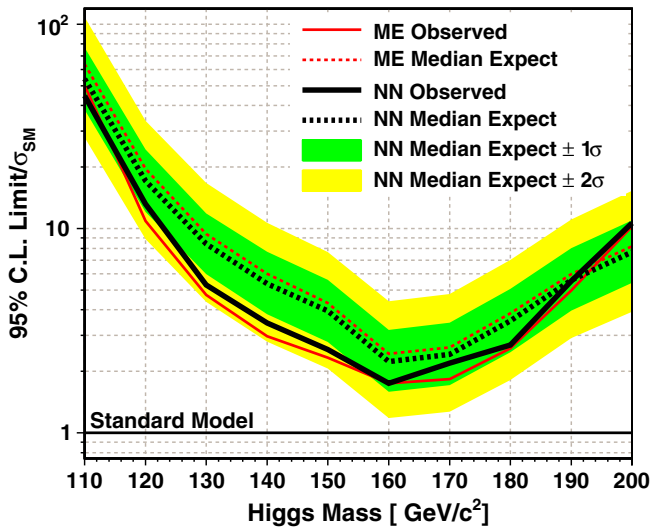
FIG. 2 (color online). Upper limits on $(\sigma \times \mathcal{B})/(\sigma \times \mathcal{B})_{\mathrm{SM}}$ versus m_H.

the $gg \rightarrow H$ coupling is enhanced by additional particles in the virtual loops of the production amplitude [18].

[a]Deceased

[b]Visitor from University of Massachusetts Amherst, Amherst, MA 01003, USA.

[c]Visitor from Universiteit Antwerpen, B-2610 Antwerp, Belgium.

[d]Visitor from University of Bristol, Bristol BS8 1TL, United Kingdom.

[e]Visitor from Chinese Academy of Sciences, Beijing 100864, China.

[f]Visitor from Istituto Nazionale di Fisica Nucleare, Sezione di Cagliari, 09042 Monserrato (Cagliari), Italy.

[g]Visitor from University of California Irvine, Irvine, CA 92697, USA.

[h]Visitor from University of California Santa Cruz, Santa Cruz, CA 95064, USA.

[i]Visitor from Cornell University, Ithaca, NY 14853, USA.

[j]Visitor from University of Cyprus, Nicosia CY-1678, Cyprus.

[k]Visitor from University College Dublin, Dublin 4, Ireland.

[l]Visitor from Royal Society of Edinburgh/Scottish Executive Support Research Fellow, United Kingdom.

[m]Visitor from University of Edinburgh, Edinburgh EH9 3JZ, United Kingdom.

[n]Visitor from Universidad Iberoamericana, Mexico D.F., Mexico.

[o]Visitor from Queen Mary, University of London, London, E1 4NS, United Kingdom.

[p]Visitor from University of Manchester, Manchester M13 9PL, United Kingdom.

[q]Visitor from Nagasaki Institute of Applied Science, Nagasaki, Japan.

[r]Visitor from University of Notre Dame, Notre Dame, IN 46556, USA.

[s]Visitor from University de Oviedo, E-33007 Oviedo, Spain.

[t]Visitor from Simon Fraser University, Vancouver, British Columbia, Canada V6B 5K3.

[u]Visitor from Texas Tech University, Lubbock, TX 79409, USA.

[v]Visitor from IFIC(CSIC-Universitat de Valencia), 46071 Valencia, Spain.

[w]University of Virginia, Charlottesville, VA 22904, USA.

[x]Visitor from University of Bologna, I-40127 Bologna, Italy.

[y]Visitor from University of Padova, I-35131 Padova, Italy.

[z]Visitor from University of Pisa, I-56127 Pisa, Italy.

[aa]Visitor from University of Siena, I-56127 Pisa, Italy.

[bb]Visitor from Scuola Normale Superiore, I-56127 Pisa, Italy.

[cc]Visitor from Sapienza Universit'a di Roma, I-00185 Roma, Italy.

[dd]Visitor from University of Trieste/Udine, Italy.

[ee]On leave from J. Stefan Institute, Ljubljana, Slovenia.

[1] R. Barate et al. (LEP Working Group for Higgs boson searches), Phys. Lett. B **565**, 61 (2003).

[2] J. Alcaraz et al. (LEP), arXiv:0712.0929.

[3] A. Djouadi, Phys. Rep. **457**, 1 (2008), see for a recent review.

[4] V. M. Abazov et al. (D0 Collaboration), Phys. Rev. Lett. **96**, 011801 (2006); A. Abulencia et al. (CDF Collaboration), Phys. Rev. Lett. **97**, 081802 (2006).

[5] D. Acosta et al. (CDF Collaboration), Phys. Rev. D **71**, 032001 (2005).

[6] D. Acosta et al. (CDF Collaboration), Phys. Rev. Lett. **94**, 091803 (2005).

[7] A. Abulencia et al. (CDF Collaboration), Phys. Rev. Lett. **98**, 161801 (2007).

[8] S. Frixione and B. R. Webber, J. High Energy Phys. 06 (2002) 029.

[9] T. Sjostrand, S. Mrenna, and P. Skands, J. High Energy Phys. 05 (2006) 026.

[10] U. Baur and E. L. Berger, Phys. Rev. D **47**, 4889 (1993).

[11] R. Brun, R. Hagelberg, M. Hansroul, and J. Lassalle, version 3.15, CERN-DD-78-2-REV.

[12] J. M. Campbell and R. K. Ellis, Phys. Rev. D **60**, 113006 (1999).

[13] M. Feindt and U. Kerzel, Nucl. Instrum. Methods Phys. Res., Sect. A **559**, 190 (2006).

[14] A. Hocker *et al.*, arXiv:physics/0703039.

[15] U. Baur, T. Han, and J. Ohnemus, Phys. Rev. D **57**, 2823 (1998).

[16] N. Kidonakis and R. Vogt, Phys. Rev. D **68**, 114014 (2003); M. Cacciari *et al.*, J. High Energy Phys. 04 (2004) 068.

[17] S. Catani, D. de Florian, M. Grazzini, and P. Nason, J. High Energy Phys. 07 (2003) 028.

[18] A. V. Manohar and M. B. Wise, Phys. Lett. B **636**, 107 (2006); G. D. Kribs, T. Plehn, M. Spannowsky, and T. M. P. Tait, Phys. Rev. D **76**, 075016 (2007).